Environ Geol (2009) 57:1893–1899
DOI 10.1007/s00254-008-1478-7

ORIGINAL ARTICLE

Sinks of iron and manganese in underground coal mine workings

Natalie A. S. Kruse · Paul L. Younger

Received: 18 February 2008 / Accepted: 7 July 2008 / Published online: 22 July 2008

Abstract The sources and sinks of manganese in underground coal mine workings are poorly understood compared to those of iron. The geochemical system in the secondary egress drift of Caphouse Colliery near Horbury, UK, is an ideal system for studying these processes. Five locations along the drift and four secondary inflows to the drift were sampled 24 times through the year commencing May 2005. During the sampling period, the pH in the main channel varied from 6.73 to 7.93 and increased along the flow path. The secondary inflows to the drift from the strata were of higher alkalinity (mean = 385 mg/L as $CaCO_3$) than the main flow (mean = 330 mg/L as $CaCO_3$); the affects of mixing between the less alkaline main channel and the more alkaline secondary inflows and of carbon dioxide exsolution are evident in the form of carbonate and hydroxide precipitates. SEM and XRD analysis of precipitates collected from the drift confirm the presence of calcium and manganese carbonates and ferric hydroxide. PHREEQC speciation and solubility modelling confirms supersaturation of the water in the main channel with respect to ferric oxy-hydroxides; iron, manganese, magnesium and calcium carbonates; and manganese oxides.

Keywords Coal · Mining · Manganese · Iron · Water · UK

Electronic supplementary material The online version of this article (doi:10.1007/s00254-008-1478-7) contains supplementary material, which is available to authorized users.

N. A. S. Kruse (✉) · P. L. Younger
Hydrogeochemical Engineering Research and Outreach,
Sir Joseph Swan Institute for Energy Research,
Newcastle University,
Newcastle upon Tyne NE1 7RU, UK
e-mail: natalie.kruse@ncl.ac.uk

Introduction

Mine closures continue to create new pollutant discharges; characterization of the source of mine water is key in the approximation of longevity of pollution (Younger 1997). Since many mines are driven either below natural groundwater level (Adams and Younger 2001) or in incompetent strata (Crowell 2001) and may have mine gas hazards in the absence of artificial ventilation (Hall 2007), opportunities for underground characterization are limited.

Iron is commonly found in mine waters and is usually taken to be a product of weathering of iron sulphides. Pyrite (FeS_2) weathering is seen as the most common source of iron in many mine systems, especially from abandoned coal mines, and the series of weathering reactions have been studied extensively (e.g. Wiersma and Rimstidt 1984; McKibben and Barnes 1986; Rimstidt and Newcomb 1993; Williamson and Rimstidt 1994; Holmes and Crundwell 2000).

Sinks of manganese in natural aquatic systems are less well defined than sources of iron. Iron oxy-hydroxide precipitates are a common sink of iron, although the precipitation reaction releases acidity. Efflorescent ferrous/ferric hydroxysulphate salts are less-well studied, but can be significant sinks for metals including iron, especially in underground mines where there is insufficient water to transport the products of mineral weathering away from the mineral surface (Younger et al. 2002), or where mine water can evaporate to dryness.

Black substrates associated with mine waters are generally attributed to manganese-rich precipitates, although some more crystalline ferric hydroxide salts are also black. Oxidation and hydrolysis of manganese gives rise to manganese oxides and hydroxides (e.g. pyrolusite and pyrochroite). The appropriate geochemical conditions can

also give rise to the precipitation of manganese carbonate, rhodochrosite, and a siderite-rich solid solution of siderite and rhodochrosite (Blowes et al. 2003).

This paper presents a characterization of the sources and sinks of iron and manganese in an abandoned underground coal mine, Caphouse Colliery, located in Yorkshire, UK. As access to these workings has been maintained to allow part of them to be used as a museum, the site offers a rare opportunity to gain insight into geochemical processes that occur in abandoned underground mines.

Site description and mining history

Caphouse Colliery is located near Horbury, West Yorkshire in northern England (Fig. 1). Caphouse Colliery was mined until the mid-1980s as part of a complex of mines including Denby Grange and Woolley Collieries. After closure, in 1985, conversion of the colliery into a museum commenced. The Yorkshire Mining Museum opened on the site in 1988 and was given status as the National Coal Mining Museum for England in 1995.

Water from abandoned workings is pumped from the adjacent Hope Shaft in order to keep the underground exhibits dry. Drainage originating in the secondary egress drift (1 in 4) (maintained to act as an emergency exit from the museum) is one of several sources of water reporting to the pumps at Hope Shaft. The secondary egress drift (see Fig. 2) consists of two legs, approximately 250 m in length each, with a nearly 180° direction change between the two legs. The secondary egress drift workings are safely accessible without disturbing museum visits, and it was therefore used for the characterization of mine water at the site.

Caphouse Colliery is developed within Lower and Middle Coal Measures strata of Carboniferous age. The average regional dip is 3°–5° to the south east, although locally significant faulting alters the dip. Typical cyclothemic sequences predominate, comprising interbedded sandstones, siltstones, mudstones, coals and seat earths (Foster 2005).

Hydrogeologically, the mine workings are the only significant groundwater system in the area; natural groundwater drainage potential is very restricted. The extensive fault system often acts as a hydrologic barrier between workings (Foster 2005). The site drains generally from west to east; the main receiving waters are the River Calder in the North and the River Dearne in the South.

The River Calder Valley was extensively mined for several hundred years. The strata generally dip from the northwest to the southeast. This has resulted in a progression of mining over time from the shallower coal seams in the northwest to the deeper seams in the southeast. Generally, the mines in the northwest of the valley (e.g. Gregory Springs) are shallower, older and tend to have been mined by room and pillar methods, while the mines in the southeast of the valley (e.g. Woolley Colliery) are deeper, newer and tend to have been mined by longwall methods (Foster 2005).

A plan dated 1791, showing workings from 1789 and planned workings up to 1795, includes a shaft on the Caphouse site, although mining probably started from the drift entrances long before the shaft was sunk. This shaft is now the oldest coal-mine shaft still in everyday use in Britain (Schofield 2003). By 1985 the economically viable coal at Caphouse Colliery was exhausted and its conversion to a museum began. Through the life of the mine, the Flockton Thick seam, the Flockton Thin Seam, the Old Hards seam, the Green Lane Seam, the New Hards Seam, the Wheatley Lime Seam, the Blocking Seam, and the Beeston Seam were all mined from the shaft at Caphouse (Goodchild 2000). Figure 3 shows a geological cross-section of the Coal Measures strata at Caphouse Colliery.

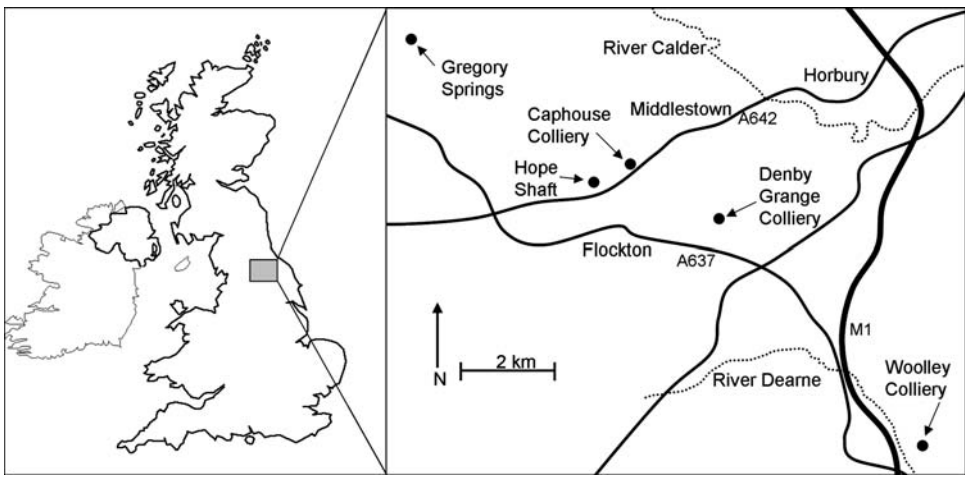

Fig. 1 Location of study site

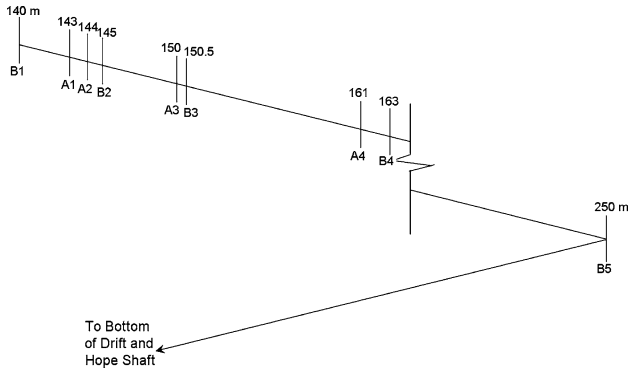

Fig. 2 Location of sampling points along the drift

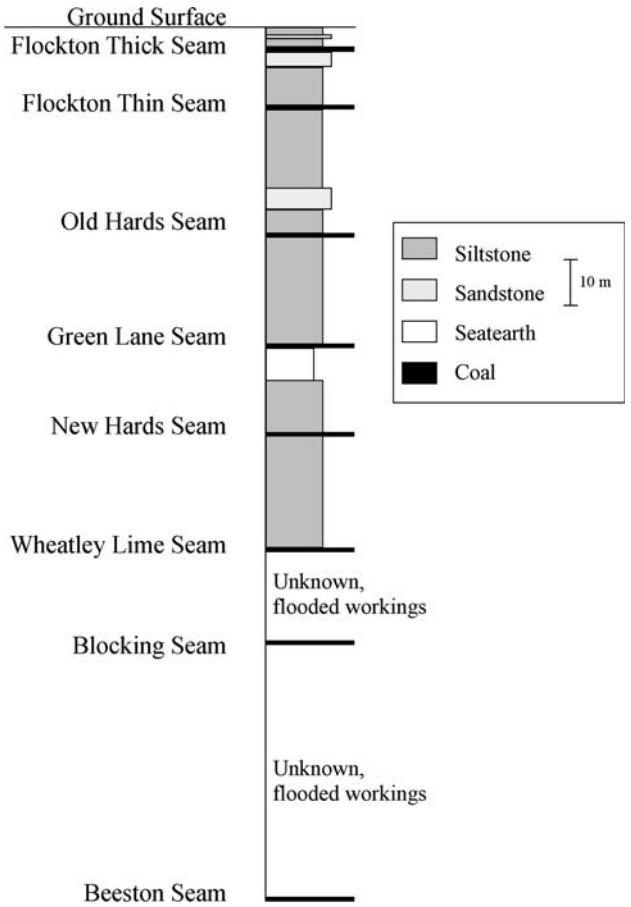

Fig. 3 Geological cross-section of Coal Measures strata at Caphouse Colliery, UK

After initial closure in 1985, pumping of Caphouse Colliery from Hope Shaft was discontinued, and ongoing pumping at Woolley Colliery was sufficient at first to maintain water levels below the level of the mining museum. Mine water abstraction from Woolley Colliery continued to maintain the water levels below the underground museum for 10 years after Woolley Colliery closed (in 1987) until water levels at Caphouse began to rise, implying a reduction in hydraulic connectivity between Caphouse and Woolley Collieries, probably due to partial collapse of the single major roadway connecting the two. After a period of investigation, pumping from the Hope Shaft was resumed in 1997 to ensure the future of the museum.

In order to treat the ferruginous water pumped from Hope Shaft, two reed beds were installed on site and commissioned in October 2003. During 2004, the water pumped from Hope Shaft contained, on average, 15.6 mg/L total iron, 0.90 mg/L total manganese, 1,147 mg/L sulphate, and had a pH of 6.88 (Foster 2005).

A substantial element of the maintenance work in the mine is devoted to keeping the secondary egress drift easily passable for emergency use. Throughout the sampling period, strata settlement and small rock collapses were observed—these were promptly reinforced with new steel rings. Water entering the drift is diverted by means of a half-pipe channel (8 in. in diameter) running the length of the drift. Drippers are intercepted with plastic sheeting and pipes to divert them into this channel. The water is then piped to flooded workings which are subsequently pumped to the surface for treatment either at Hope Shaft or Woolley Colliery.

Sampling and analysis methods

At each sample collection point, measurements of temperature, pH, Eh, electrical conductivity and alkalinity were made using a Myron 6P Ultrameter (temperature, pH, Eh and conductivity) and a Hach digital titrator (alkalinity concentration), which were calibrated before each visit. The Hach digital titrator was used with 1.6 N sulphuric acid and Bromcresol-Green Methyl-Red indicator powder, to give results in units of mg/L as $CaCO_3$. Samples for laboratory analysis were collected in pre-washed polyethylene bottles. One hundred and twenty-five millilitres bottles pre-acidified with lab-grade concentrated hydrochloric acid were used for collection of samples for analysis of metals. Unacidified 125-mL bottles were used for collection of samples for analysis of chloride and sulphate. All metals were analysed using a Varian Vista-MPX ICP-OES; blanks and standards were run periodically to ensure QA/QC of metals analyses. Anions were analysed using a Dionex 100 Ion Chromatographion; standards were run to ensure QA/QC of the analysis.

Distributed underground samples were collected weekly for the first 3 months, fortnightly for the following 7 months and monthly for a further 2 months. Distance from the ventilation doors at the top of the drift to each sample point was measured using a distance measuring wheel. The exact point of sample collection for each

location was marked to ensure consistency of sampling. Immediately after sample collection, temperature, pH, Eh and conductivity were measured as detailed above. Alkalinity for all samples was analysed after returning to the surface, always within an hour of sample collection. Samples were stored at 4°C within 5 h of collection until analysis. Analysis was performed within a week of sample collection.

The secondary inflow samples include two "feeders" (i.e. point inflows, resembling underground springs, that often contribute the bulk of water entering a mine (Younger et al. 2002); one "dripper" (i.e. diffuse water input in the form of drops falling from the ceiling (Younger et al. 2002); and one secondary floor channel. A1 is the dripper, A2 and A4 are feeders and A3 is the secondary floor channel.

The nine sampling points along the first 250 m of the secondary egress drift at Caphouse Colliery are shown graphically in Fig. 2. Eight of these are within an especially wet area of the drift and are spaced within a length of 20 m; four of these are feeders, drippers or secondary inflows and four are sampling points within the main channel of flow. The ninth sampling point is at the bottom of the first leg of the drift, approximately 150 m down flow from the other eight samples. The inflow samples are labelled with an A (e.g. A1) and the main channel samples are labelled with a B (e.g. B1).

The limitations of underground sampling have led to possible sources of error. Samples were not filtered due to limited time for sampling and replicate samples were not taken. Additionally, the time between sampling and alkalinity analysis could have affected the results of the analysis. Sources of this error could be due to CO_2 off gassing, precipitation of carbonate species, interactions that cause transformation of base cations and biological activity. The time elapsed before samples were refrigerated is an additional source of possible error. Electroneutrality of each sample was calculated; any sample with an electroneutrality of greater than 10% or less than −10% was neglected. Standard QA/QC procedures were used in lab analysis; blanks and standards were run periodically and each sample was analysed in triplicate to minimize error in measurement.

Mine water chemistry

Although a full suite of metals and anions were analysed, only a few were found in measurable quantities to warrant discussion. Both the main channel and the secondary inflows tend to be circum-neutral (varying from 6.73 to 7.93) with moderate iron (varying from <0.01 to 78.0 mg/L) and manganese (varying from 0.02 to 2.4 mg/L) concentrations. The mean water chemistry data for each sample location are included in Table 1; a full suite of water chemistry data is included in the supplementary information. All but two samples were either at or below detection limit for As (0.05 mg/L), Cd (0.01 mg/L), Co (0.01 mg/L), Cr (0.01 mg/L), Cu (0.01 mg/L), Ni (0.01 mg/L) and Pb (0.1 mg/L).

The main channel becomes more alkaline along its length (Fig. 4). The secondary inflows tend to have higher alkalinities than those measured in the main channel so that as they combine with the main flow, they add alkalinity to the water in the main channel. The secondary inflows associated with sample points A1, A3, and A4 have sufficient time before mixing into the main channel to oxidize and off-gas CO_2 before both sampling and mixing with the main channel. The inflow corresponding to sample point A2, however, was sampled at the point where water met the

Table 1 Summary of mean water chemistry for sample period of May 2005–May 2006 for each of nine sample points in the secondary egress drift for Caphouse Colliery, UK

Sample	Alk (mg/L $CaCO_3$)	Cl^- (mg/L)	SO_4^{2-} (mg/L)	Ca (mg/L)	Mg (mg/L)	Fe (mg/L)	Mn (mg/L)	Al (mg/L)	Zn (mg/L)	Temp (°C)	Eh (mV)	pH (°)
Inflows												
A1	379.17	67.61	288.22	164.22	77.04	1.31	0.77	0.5	0.03	11.42	134.45	6.96
A2	397.43	76.65	396.13	200.83	88.13	2.73	0.47	<0.1	0.03	10.78	17.64	6.93
A3	359.09	67.43	338.17	180.78	81.32	0.43	0.50	0.1	0.02	10.62	18.73	7.81
A4	400.23	72.09	350.77	186.22	86.74	0.93	0.47	<0.1	0.03	10.65	1.53	7.29
Main channel												
B1	267.09	97.18	425.22	163.74	86.37	11.79	1.32	0.5	0.03	11.31	5.09	7.14
B2	325.78	80.39	352.61	163.22	80.73	2.74	0.90	0.2	0.02	10.84	13.27	7.30
B3	355.86	78.30	352.96	172.30	81.42	1.47	0.59	0.1	0.03	10.49	−55.27	7.55
B4	357.65	73.78	353.78	173.17	82.19	1.29	0.61	0.1	0.02	10.50	−18.36	7.50
B5	338.33	71.87	349.27	167.47	79.78	2.13	0.59	0.1	0.02	10.27	−28.82	7.75

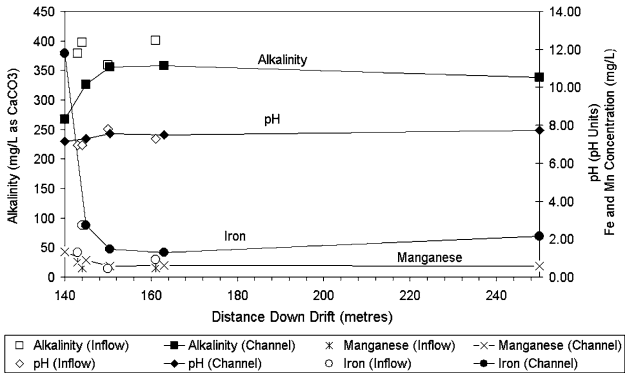

Fig. 4 Effect of secondary inflows on alkalinity, pH, and iron and manganese concentrations along the length of the drift. *Open symbols* represent the chemistry of secondary inflows while *solid symbols* connected by *lines* represent the chemistry of the main channel

atmosphere and, based on the work of Hall (2007), before meeting the atmosphere, the water contained significant concentrations of CO_2 ($pCO_{2water} = 5 \times pCO_{2atmosphere}$) (Hall 2007). For the area surrounding this sample point, it is likely that changes in water chemistry and carbonate precipitation is due to CO_2 loss rather than mixing. This is also reflected in downstream increase in pH (Fig. 4). As would be expected, the rise in pH correlates with evidence for precipitation of metals. The pH rise is evident in declines in concentrations of manganese and iron (Fig. 4). Iron oxy-hydroxide and manganese carbonate precipitates become conspicuous below 145 m down drift. Calcium carbonate precipitates are visibly abundant below 147 m down drift. The precipitation of calcium carbonates accounts for lower calcium concentrations in the main flow despite higher calcium concentrations in the secondary inflows (see Table 1). This is also a likely mechanism for maintained levels of alkalinity after an large increase above sample point A2 (see Fig. 4), visible evidence of calcium carbonate precipitates between sample points A2 and A4 support this theory. Eh–pH diagrams for iron, manganese and calcium minerals are presented in Fig. 5 and are discussed below.

Mineralogical analyses

Several precipitates gathered from between 145 and 160 m down the secondary egress drift from the surface were analysed using SEM and XRD. Two results came from this analysis—first, abundance of calcium and manganese carbonates and, second, layered precipitation of calcite on calcite (Fig. 6a) and of manganese carbonate on calcite (Fig. 6b). Mineralogical analysis of precipitates showed co-precipitation of calcite and aragonite, both will be referred to here as calcium carbonates. The calcium carbonates precipitated below the manganese carbonate was precipitated in layers as well. The calcium carbonates and manganese carbonate precipitate group was gathered as a thin (2.5 cm thick) layer precipitated on a plastic sheet. The XRD analysis also revealed a possible solid solution of a manganese-rich carbonate into a dolomite structure.

Discussion of results

Although the water samples tested were all circum-neutral, a significant difference is seen between the alkalinity of the secondary inflows, especially A2 and A4, and that of the main channel. The increased alkalinity of these inflows

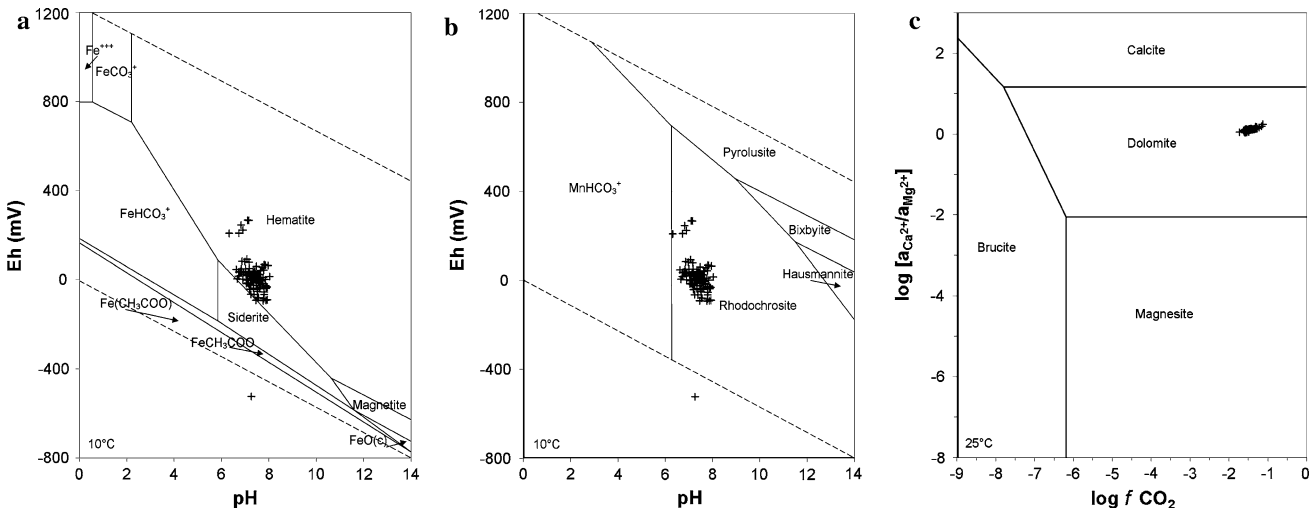

Fig. 5 Eh–pH and activity diagrams demonstrating solubility fields of geochemical species for waters flowing in Caphouse Colliery for **a** Fe–O–H–C, **b** Mn–O–H–C, and **c** Ca–Mg–O–H–C (Marini 2007) systems. All plots are for pressure equal to 1.013 bar

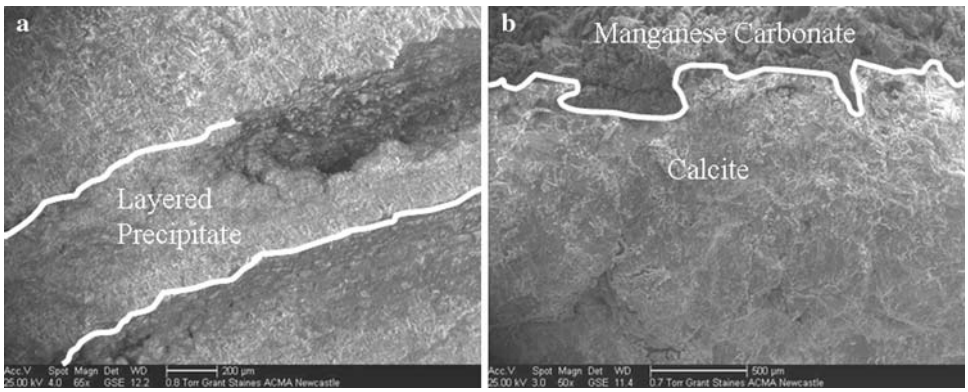

Fig. 6 SEM images of precipitates collected from secondary drift at Caphouse Colliery. **a** Layered precipitation of calcite on calcite; **b** sequential precipitation of calcite followed by manganese carbonate

Table 2 Saturation phases of relevant solid phases as calculated with PHREEQC for average aqueous chemistry of each sample for the year commencing May 2005

	Saturation indices of inflows				Saturation indices of main channel				
	A1	A2	A3	A4	B1	B2	B3	B4	B5
Anhydrite	1.01	1.16	1.09	1.1	1.13	1.07	1.08	1.08	−1.16
Aragonite	2.2	2.22	3.01	2.56	2.17	2.44	2.73	2.69	0.57
Calcite	2.35	2.37	3.16	2.71	2.32	2.59	2.89	2.84	0.72
$CO_2(g)$	0.11	0.14	−0.8	−0.21	−0.24	−0.31	−0.53	−0.47	−2.26
Dolomite	4.31	4.33	5.92	5.03	4.31	4.82	5.39	5.31	1.25
$Fe(OH)_3(a)$	2.11	2.33	4.11	2.91	3.7	3.48	3.93	3.68	3.75
Goethite	7.45	7.67	9.44	8.25	9.04	8.81	9.26	9.02	9.08
Gypsum	1.25	1.4	1.33	1.34	1.37	1.31	1.33	1.33	−0.9
$H_2(g)$	−21.92	−21.86	−23.62	−22.58	−22.28	−22.6	−23.1	−23	−23.48
$H_2O(g)$	−1.92	−1.93	−1.92	−1.92	−1.92	−1.92	−1.92	−1.92	−1.92
Hausmannite	−15.37	−16.24	−9.68	−13.56	−12.95	−12.44	−11.24	−11.58	−11.48
Haematite	16.84	17.28	20.82	18.43	20.01	19.57	20.46	19.98	20.09
Manganite	−5.17	−5.47	−2.99	−4.45	−4.3	−4.08	−3.6	−3.73	−3.61
Melanterite	−3.56	−3.15	−4.06	−3.69	−2.36	−3.13	−3.43	−3.53	−5.58
$O_2(g)$	−44.6	−44.72	−41.2	−43.28	−43.88	−43.24	−42.24	−42.44	−41.47
Pyrochroite	−5.99	−6.26	−4.66	−5.6	−5.3	−5.24	−5.01	−5.09	−5.21
Pyrolusite	−12.78	−13.11	−9.74	−11.73	−11.73	−11.35	−10.61	−10.79	−10.44
Rhodochrosite	2.18	1.94	2.61	2.24	2.51	2.51	2.53	2.5	0.59
Siderite	2.14	2.42	2.37	2.28	3.19	2.74	2.72	2.58	0.61

buffers the main channel flow, increasing its alkalinity and allowing metals to precipitate—a marked decrease is seen in both the iron and manganese concentrations in the main channel after addition of the higher alkalinity inflows. The increased alkalinity in inflows A2 and A4 points to the character of the source of water flowing from these feeders. Unlike other coalfields further north in England, there is interbedding of limestones in the Westphalian in this region (Foster 2005), and some may be present at the ultimate sources of feeders A2 and A4.

The layered precipitates shown in Fig. 6b may be a result of long term water chemistry changes. The manganese carbonate precipitates are mineralogically distinct from the calcium carbonates upon which they have been precipitated showing a discontinuity in precipitation. This suggests that at some time in the recent past calcium concentrations in feeder A4 (the source of the precipitates) decreased to below the solubility limit and manganese concentrations increased enough to begin precipitating manganese carbonate.

Although manganese oxides and hydroxides are considered by Blowes et al. (2003) to be the more likely form for manganese sinks in oxic systems (Blowes et al. 2003), this was not the case at Caphouse. The dominance of

dissolved carbonate in the system led to the preferential precipitation of manganese carbonates. Unexpectedly, this did not hold for iron sinks which were predominantly iron oxy-hydroxides. This is probably due to the smaller differences between the solubility of iron oxy-hydroxides and siderite than that between manganese oxides (pyrolusite and pyrochroite) and rhodochrosite (Stumm and Morgan 1996). This highlights the need for mineralogical analysis of precipitates and modelling sites using software such as PHREEQC for a more complete understanding of the controlling chemistry of a site (Table 2).

In the Eh–pH diagrams presented in Fig. 5, all samples plot close to the boundary line between siderite and haematite for the Fe–O–H–C system (Fig. 5a) and well within the predominance field for rhodochrosite on the Mn–O–H–C system (Fig. 5b). Under the assumption of redox equilibrium, these plots support the precipitation of rhodochrosite, while the precipitation of an oxy-hydroxide of Fe^{3+} (represented by the Haematite stability field) rather than siderite may be explained by either solid solution of oxy-hydroxides instead of pure haematite, thus enlarging the haematite stability field or for kinetic reasons (a limitation of the assumption of redox equilibrium). All water samples plot well within the dolomite field in the Ca–Mg–O–H–C activity diagram (Fig. 5c), while the field sampling showed a predominance of calcium carbonate precipitates. The stability fields on these diagrams are based on thermodynamic grounds, but here the predominance of kinetic controls on precipitates is seen. Precipitation of Ca carbonates is more kinetically favourable than that of dolomite (Marini 2007).

Conclusions

Caphouse Colliery provides an interesting case study of subsurface water quality and hydrogeology. There are few opportunities for sample collection in underground mines—this characterization shows some of the unique geochemical processes taking place in underground mines.

The water collected from Caphouse Colliery's secondary drift was circum-neutral with detectable levels of iron, manganese, aluminium and zinc. Feeders and drippers affect the chemistry of the main channelized flow, generally through alkaline addition.

References

Adams R, Younger PL (2001) A strategy for modelling ground water rebound in abandoned deep mine systems. Ground Water 39(2):249–261

Blowes DW, Ptacek CJ, Jambor JL, Weisener CG (2003) The geochemistry of acid mine drainage. In: Holland HD, Turekian KK (eds) Treatise on geochemistry, vol 9. Elsevier-Pergamon, Oxford, pp 149–204

Crowell DL (2001) Mine subsidence. Division of Geological Survey, Ohio Department of Natural Resources

Foster SM (2005) Integrated water management in former coal mining regions: guidance to support strategic planning. Mineral Industry Research Organization (LIFE02 ENV/UK/000140), Leeds

Goodchild J (2000) A new history of Caphouse colliery and Denby grange collieries. Wakefield Historical Publications, Wakefield

Hall J (2007) Sources and pathways of hazardous gases in disused mine workings. Thesis, Newcastle University

Holmes PR, Crundwell FK (2000) The kinetics of the oxidation of pyrite by ferric ions and dissolved oxygen: an electrochemical study. Geochim Cosmochim Acta 64(2):263–274

Marini L (2007) Geological sequestration of carbon dioxide: thermodynamics, kinetics, and reaction path modelling. Elsevier Science, Amsterdam

McKibben MA, Barnes HL (1986) Oxidation of pyrite in low temperature acidic solutions: rate laws and surface textures. Geochim Cosmochim Acta 50:1509–1520

Rimstidt JD, Newcomb WD (1993) Measurement and analysis of rate data: the rate of reaction of ferric iron with pyrite. Geochim Cosmochim Acta 57(9):1919–1934

Schofield J (2003) Caphouse colliery: a brief mining history. National Coal Mining Museum for England, Wakefield

Stumm W, Morgan JJ (1996) Aquatic chemistry chemical equilibria and rates in natural waters. Wiley, New York

Wiersma CL, Rimstidt JD (1984) Rates of reaction of pyrite and marcasite with ferric iron at pH 2. Geochim Cosmochim Acta 48:85–92

Williamson MA, Rimstidt JD (1994) The kinetics and electrochemical rate-determining step of aqueous pyrite oxidation. Geochim Cosmochim Acta 58(24):5443–5454

Younger PL (1997) The longevity of minewater pollution: a basis for decision-making. Sci Total Environ 194(195):457–466

Younger PL, Banwart S, Hedin RS (2002) Mine water: hydrology, pollution, remediation. Kluwer Academic Publishers, London